

AD-A067 629

AEROSPACE CORP EL SEGUNDO CALIF IVAN A GETTING LABS F/6 9/1  
TRANSIENT RADIATION AND DOSE-ENHANCEMENT EFFECTS IN TRANSISTORS--ETC(U)  
AUG 78 G M MOLEN, M J BERNSTEIN, K W PASCHEN F04701-77-C-0078  
TR-0078(3950-04)-4 SAMSO-TR-78-108 NL

UNCLASSIFIED

| OF |

AD  
A067629



END  
DATE  
FILMED  
6-79  
DDC

LEVEL #

4

ADA067629

DDC FILE COPY

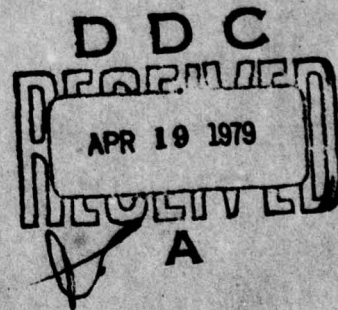
## Transient Radiation and Dose-Enhancement Effects in Transistors

G. M. MOLEN, M. J. BERNSTEIN, K. W. PASCHEN, and R. H. VANDRE  
Materials Sciences Laboratory  
The Ivan A. Getting Laboratories  
The Aerospace Corporation  
El Segundo, Calif. 90245

22 August 1978

Interim Report

APPROVED FOR PUBLIC RELEASE;  
DISTRIBUTION UNLIMITED



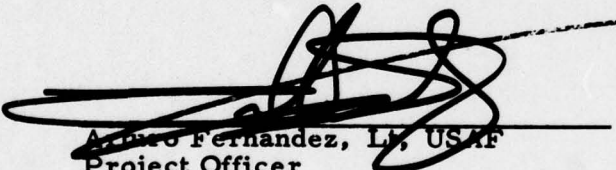
Prepared for  
SPACE AND MISSILE SYSTEMS ORGANIZATION  
AIR FORCE SYSTEMS COMMAND  
Los Angeles Air Force Station  
P.O. Box 92960, Worldway Postal Center  
Los Angeles, Calif. 90009

78 10 02 046


This interim report was submitted by The Aerospace Corporation, El Segundo, CA 90245, under Contract No. F04701-77-C-0078 with the Space and Missile Systems Organization, Deputy for Advanced Space Programs, P.O. Box 92960, Worldway Postal Center, Los Angeles, CA 90009. It was reviewed and approved for The Aerospace Corporation by W. C. Riley, Director, Materials Sciences Laboratory. Lieutenant Arturo Fernandez, SAMSO/YCPT, was the project officer for Advanced Space Programs.

This report has been reviewed by the Information Office (OI) and is releasable to the National Technical Information Service (NTIS). At NTIS, it will be available to the general public, including foreign nations.

This technical report has been reviewed and is approved for publication. Publication of this report does not constitute Air Force approval of the report's findings or conclusions. It is published only for the exchange and stimulation of ideas.



Arturo Fernandez, Lt, USAF  
Project Officer



Robert W. Lindemuth, Lt Col, USAF  
Chief, Technology Plans Division

FOR THE COMMANDER



LEONARD E. BALTZELL, Col, USAF  
Asst Deputy for Advanced Space Programs

UNCLASSIFIED

SECURITY CLASSIFICATION OF THIS PAGE (When Data Entered)

19 REPORT DOCUMENTATION PAGE		READ INSTRUCTIONS BEFORE COMPLETING FORM	
1. REPORT NUMBER	2. GOVT ACCESSION NO.	3. RECIPIENT'S CATALOG NUMBER	
18 6 SAMSO-TR-78-108		9	
4. TITLE (and Subtitle)		5. TYPE OF REPORT & PERIOD COVERED	
TRANSIENT RADIATION AND DOSE- ENHANCEMENT EFFECTS IN TRANSISTORS		Interim <i>rept</i>	
7. AUTHOR(s)		6. PERFORMING ORG. REPORT NUMBER	
10 G. Marshall Molen, Melvin J. Bernstein, Kenneth W. Paschen, and Robert H. Vandre		14 TR-0078(3950-04)-4	
		8. CONTRACT OR GRANT NUMBER(s)	
		15 F04701-77-C-0078	
9. PERFORMING ORGANIZATION NAME AND ADDRESS		10. PROGRAM ELEMENT, PROJECT, TASK AREA & WORK UNIT NUMBERS	
The Aerospace Corporation El Segundo, Calif. 90245			
11. CONTROLLING OFFICE NAME AND ADDRESS		12. REPORT DATE	
Space and Missile Systems Organization Air Force Systems Command Los Angeles, Calif. 90009		11 22 August 1978	
14. MONITORING AGENCY NAME & ADDRESS (if different from Controlling Office)		13. NUMBER OF PAGES	
12/36p.		31	
		15. SECURITY CLASS. (of this report)	
		Unclassified	
		15a. DECLASSIFICATION/DOWNGRADING SCHEDULE	
16. DISTRIBUTION STATEMENT (of this Report)			
Approved for public release; distribution unlimited			
17. DISTRIBUTION STATEMENT (of the abstract entered in Block 20, if different from Report)			
18. SUPPLEMENTARY NOTES			
19. KEY WORDS (Continue on reverse side if necessary and identify by block number)			
Bipolar Technology Electron Transport Code Photon Interaction Radiation Environment			
20. ABSTRACT (Continue on reverse side if necessary and identify by block number)			
<p>The response of bipolar transistors to ionizing radiation is considered for a relatively soft x-ray spectrum. A plasma-focus device was used to irradiate several silicon transistors under controlled conditions so that the relative contributions to the radiation response could be isolated. The photo-current response resulting from direct photon interaction with the silicon chip was in excellent agreement with computations made on the basis of device geometry; however, contributions from packaging effects were found to be less</p>			

DD FORM 1473  
(FACSIMILE)

409944

UNCLASSIFIED

SECURITY CLASSIFICATION OF THIS PAGE (When Data Entered)

B

UNCLASSIFIED

SECURITY CLASSIFICATION OF THIS PAGE(When Data Entered)

19. KEY WORDS (Continued)

20. ABSTRACT (Continued)

predictable. The high Z package resulted in a nonuniform dose deposition in the device. The resultant dose enhancement is compared with integrated depth-dose profiles calculated with a Monte Carlo electron transport code.

UNCLASSIFIED

SECURITY CLASSIFICATION OF THIS PAGE(When Data Entered)

## PREFACE

The authors gratefully acknowledge the assistance of W. L. Chadsey and V. W. Pines of Science Applications, Inc., for performing the dose-enhancement calculation with the POEM computer program. Theoretical support was provided by R. Wilson and P. Garner of TRW Systems. G. M. Molen's present address is: ESCO Manufacturing Company, P.O. Box 1039, Greenville, Texas. M. J. Bernstein's present address is: Stanford Research Institute, 333 Ravenswood Ave., Menlo Park, California. R. H. Vandre's present address is: 5890-B Adams St., Ft. Knox, Kentucky.

ADDITIONAL INFO	
NOTE	WIND DIRECTION <input checked="" type="checkbox"/>
CRU	DAY DIRECTION <input type="checkbox"/>
UNDESIRABLE	<input type="checkbox"/>
INDICATION	
DT	
DISTRIBUTION/AVAILABILITY CODES	
Dist. Avail. Ref. or Special	
A	

# CONTENTS

PREFACE .....	1
I. INTRODUCTION.....	9
II. PHOTOCURRENT RESPONSE IN BIPOLAR TRANSISTORS ...	11
III. RADIATION-TRANSPORT CALCULATION .....	15
IV. EXPERIMENTAL DESCRIPTION .....	21
V. RADIATION STUDIES .....	25
A. Photocurrent Response Without Dose Enhancement ....	26
B. Photocurrent Response With Dose Enhancement.....	29
C. Comparison of Calculated and Measured Dose- Enhancement Factor .....	31
VI. CONCLUSION .....	35
REFERENCES .....	37
APPENDIX: COMPARISON WITH A HIGH-ENERGY RADIATION SOURCE .....	39

## FIGURES

1.	Designation of $I_{pp}$ and Secondary $I_{sp}$ Photocurrents in Bipolar Transistor .....	12
2.	Geometrical Description of Epitaxial Transistors .....	13
3.	Energy Deposition in Si Near Ni Interface .....	16
4.	Energy Deposition in Si Near Ta Interface .....	17
5.	X-Ray Energy Spectra of Plasma Focus .....	19
6.	Layout of Radiation-Response Test Fixture .....	22
7.	Electrical Circuit for Radiation Tests .....	23
8.	Radiation Test Results for 2N3947 Transistor .....	27
9.	Radiation Test Results for 2N1613 Transistor .....	28
10.	Current Injection Circuit and Test Transistor .....	30
11.	2N1613 Dose-Enhancement from 0.0002 in. Ta with Spectrum I (0.4 cm Al filtration) .....	32

# TABLES

1.	Device Characteristics . . . . .	25
2.	$I_{pp}$ at $10^8$ rad(Si)/sec Without Dose-Enhancement Effects . . . .	29
3.	Measured Dose-Enhancement Factors . . . . .	30

## I. INTRODUCTION

At photon energies below 1 MeV, the dose deposited in the active layers of semiconductor devices can be enhanced considerably by photoelectrons emitted from nearby higher Z surfaces. The most common example is the Kovar can-encapsulating transistor devices, although thin gold coatings are often encountered also. The nature of nonequilibrium radiation-dose distributions at material interfaces has been studied<sup>1,2</sup> with pulsed radiation sources; however, the experiments have been limited to relatively hard x-ray spectra. Results are reported here for the more realistic simulation spectrum from a plasma focus. The results are especially significant because of the spectral dependence of the dose-enhancement factor.

Several high-speed bipolar transistors were irradiated with the Aerospace plasma-focus devices. Carefully controlled experiments were conducted to separate the contributions from direct-photon interactions with the silicon chip and photoemission from nearby surfaces. The relative increase in the dose deposition from the latter effect is termed the dose-enhancement factor (DEF), which is defined as the ratio of total energy deposited in an active layer by both photoelectrons and photons to the energy deposited by photons. Measurements of the nonuniform dose deposition in the device are compared with depth-dose profiles calculated with a Monte Carlo electron transport code for the plasma-focus spectrum.

The series of experiments on the bipolar transistors with the plasma focus used as a pulsed-radiation simulator also demonstrated a simple procedure for the characterization of the response of semiconductor devices to transient radiation where steady-state approximations cannot be employed. The calculation of photocurrents generated in response to ionizing radiation with pulse widths less than the minority-carrier lifetime are, in general, complex because of the difficulty in defining the effective volume. In addition,

the solution must account for the buildup of primary photocurrent as a function of time and the charging of the emitter and collector capacitances, especially for the secondary photocurrent, which is related to the transient-induced primary photocurrent by the frequency-dependent current gain of the transistor  $h_{fe}$ . Simple bench tests were devised to minimize the complexity of analysis by current injection techniques.

## II. PHOTOCURRENT RESPONSE IN BIPOLAR TRANSISTORS

The primary photocurrent  $I_{pp}$  results from minority carriers in the vicinity of the base-collector region that are swept across the junction after the production of hole-electron pairs by the ionizing radiation. Since the energy required to produce one hole-electron pair in silicon is 3.6 eV, this current is easily calculated once the active volume has been identified. The secondary photocurrent  $I_{sp}$  includes the contribution from  $I_{pp}$  plus any additional current that flows as a result of current multiplication by transistor action. The direction of flow for these two currents is shown in Fig. 1 for a NPN transistor.

The steady-state primary photocurrent is directly dependent on the dose rate  $\dot{\gamma}$  in the active collection region and is expressed as

$$I_{pp} = qg_o \dot{\gamma}V_{eff} \quad (1)$$

where  $q$  is the charge of an electron,  $g_o$  is the carrier generation rate conversion factor, and  $V_{eff}$  is the effective active volume. The factor  $g_o$  is computed for silicon as  $4.0 \times 10^{13}$  carriers/cm<sup>3</sup>-(Si)rad. The identification of the effective volume is considered for epitaxial transistors (Fig. 2). Holes and electron pairs are produced uniformly throughout the silicon; however, carriers in the highly doped emitter region are neglected because of the short diffusion length. Similarly, the maximum depth in the collector region is taken as one diffusion length  $L_c$  from the base-collector junction or to the epitaxial interface, whichever is smaller. Thus, the effective volume is

$$V_{eff} = A_c(W_b + X_c + W_c) \quad (2)$$

where  $A_c$  is the collector area,  $W_b$  is the epitaxial base width,  $X_c$  is the depletion thickness, and  $W_c$  is the epitaxial layer width below the depletion

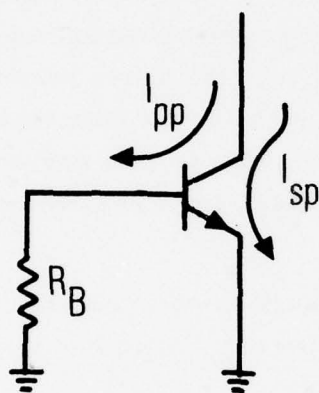


Fig. 1. Designation of  $I_{pp}$   
and Secondary  
 $I_{sp}$  Photocurrents  
in Bipolar  
Transistor

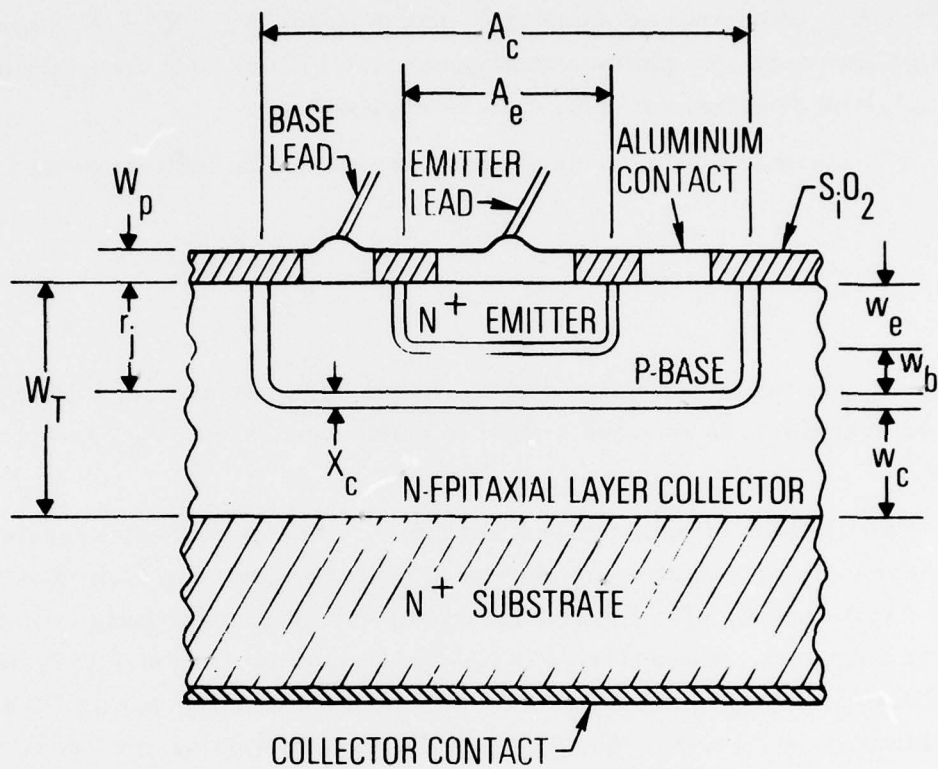


Fig. 2. Geometrical Description of Epitaxial Transistors

layer or  $L_c$ , whichever is smaller. The distance  $W_b + X_c + W_c$  represents the effective depth for photocurrent generation. Side-wall contributions to the collector area are considered to be negligible.

The steady-state secondary photocurrent can be expressed as

$$I_{sp} = (1 + h_{FE}) I_{pp} - \frac{(V_{BE} - V_{BB})h_{FE}}{R_B} \quad (3)$$

where  $V_{BB}$  is the base voltage and  $R_B$  is the base resistance.<sup>3</sup> It is assumed that the transistor is forward biased to conduction, i.e.,  $V_{BE}$  is approximately 0.7 V.

Calculations of primary and secondary transistor photocurrents in a transient ionizing radiation environment is much more complex than the steady-state solution for long radiation pulses; thus, a computer solution is usually required. Characterization of the transistor response to transient radiation requires the detailed modeling and specification of all of the internal transistor capacitances. Specifically, the current gain of the transistor  $h_{fe}$  is required to determine the secondary photocurrent, which is dependent both on the magnitude of  $I_{pp}$  and the frequency response. The frequency dependence results from the charging of the emitter and collector capacitances and the base region by the primary photocurrent. In general, the transient radiation response of the secondary photocurrent is more easily determined by simple current-injection techniques such that the induced primary photocurrent is appropriately modeled.

### III. RADIATION TRANSPORT CALCULATION

Calculations for the steady-state primary photocurrent  $I_{pp}$  can be made with the use of a simple model when secondary emission radiation effects are neglected. When these effects cannot be disregarded, it is necessary to calculate the dose-enhancement factor, which is a function of the depth-dose profile of the secondary electrons generated by nearby higher Z surfaces. The dose-enhancement factor is expressed as

$$DEF = \frac{\int_{x_1}^{x_2} [S(x) + P(x)] dx}{\int_{x_1}^{x_2} P(x) dx} \quad (4)$$

where  $x$  is the depth of penetration into the semiconductor material and the distance from  $x_1$  to  $x_2$  contains the effective volume. The function  $P(x)$  is the dose versus depth energy deposition (usually a constant) of the primary radiation in the material in which the deposition occurs, whereas  $S(x)$  is the dose versus depth profile of the secondary radiation emitted from high Z surfaces in response to the incident primary radiation. In practice, the effective volume is not uniformly sensitive to deposited carriers, and the integration limits  $x_1$  and  $x_2$  cannot be precisely determined.

The function  $S(x)$  can be determined with the use of a Monte Carlo electron transport code, POEM,<sup>4</sup> which calculates x-ray photoemission from surfaces and the depth-dose profiles in materials adjacent to photoemitting surfaces. The calculation includes the number, angle, and energy distributions of the photoelectrons emitted from a surface and also the energy and charge deposition profiles of an adjacent material. Figures 3 and 4 are

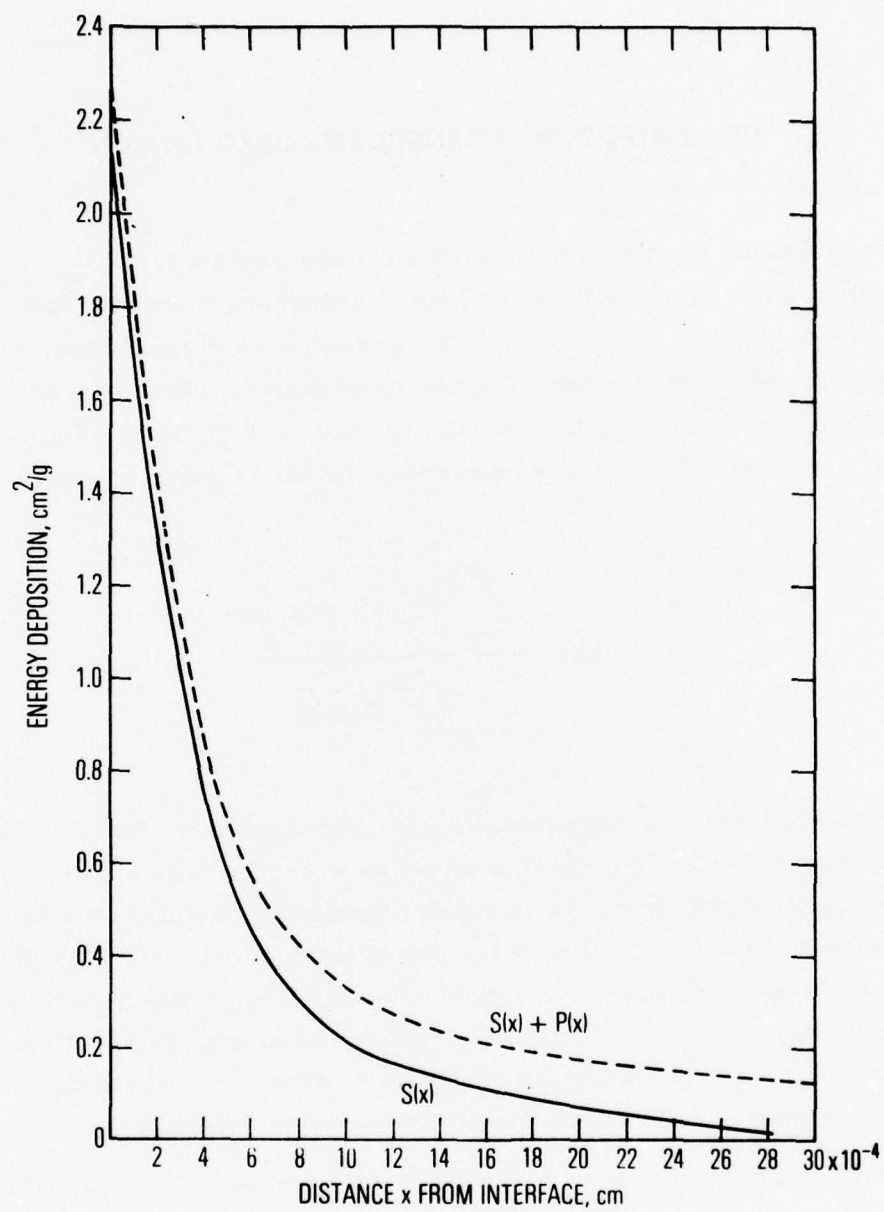


Fig. 3. Energy Deposition in Si Near Ni Interface

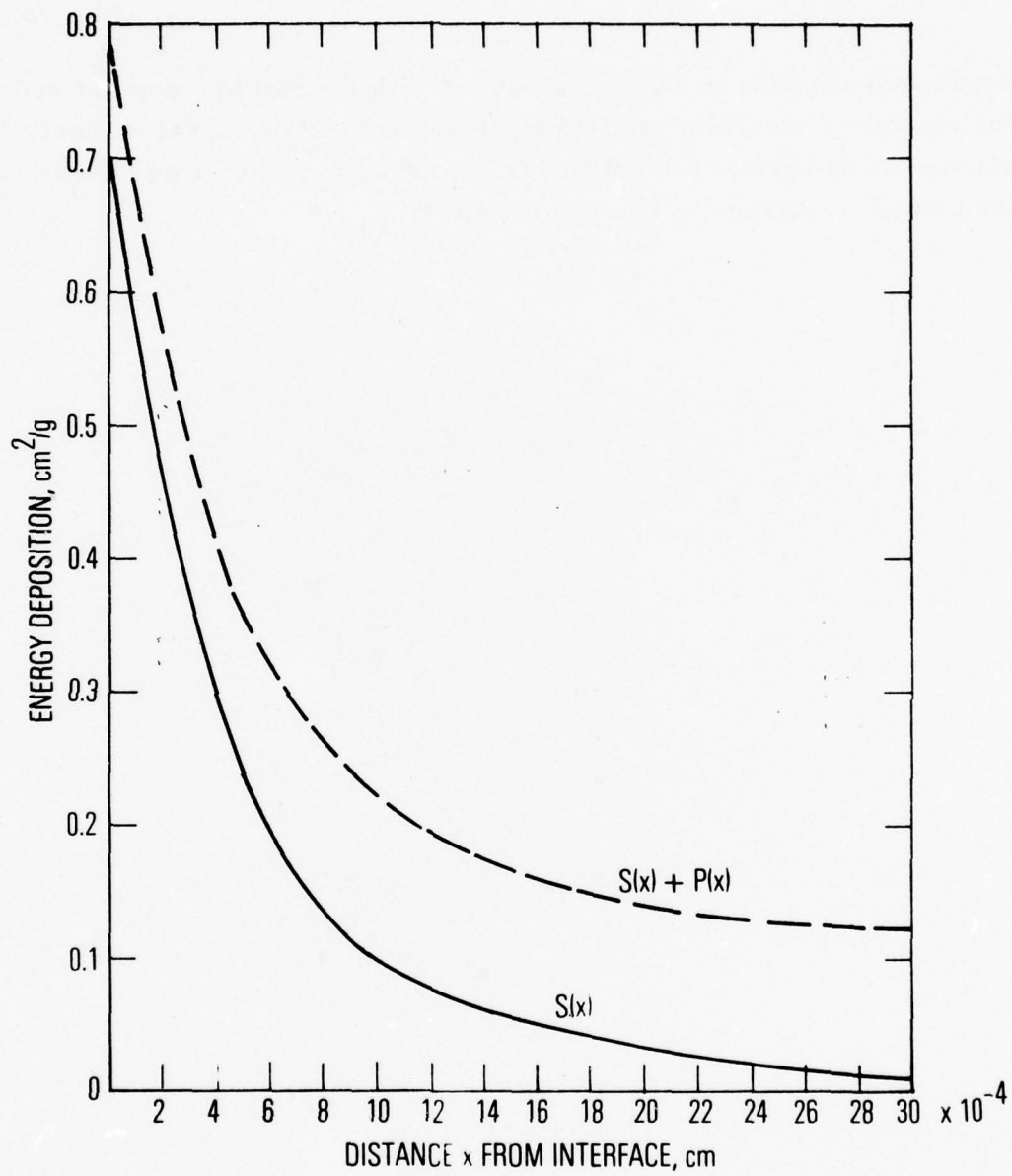


Fig. 4. Energy Deposition in Si Near Ta Interface

depth-dose profiles in silicon calculated with the POEM computer code used for secondary electrons emitted by nickel and tantalum, respectively. The plasma-focus spectrum identified in Fig. 5 as Spectrum I was used to define the primary radiation in these calculations.

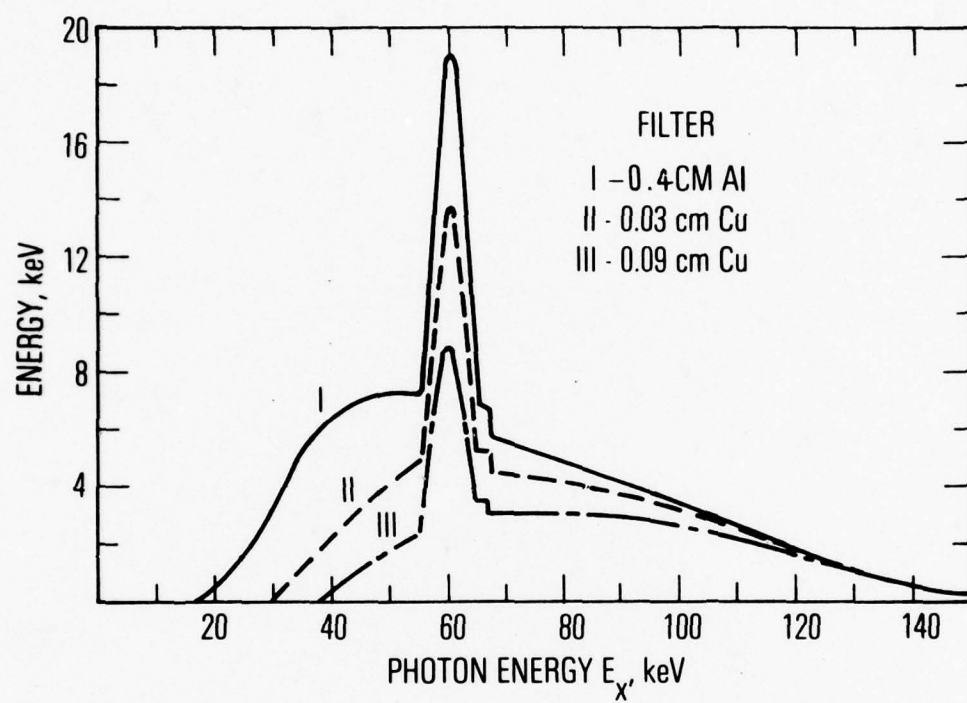


Fig. 5. X-Ray Energy Spectra of Plasma Focus

## IV. EXPERIMENTAL DESCRIPTION

Radiation tests were performed with pulsed x-ray emission from the Aerospace 34- and 140-kJ plasma-focus devices. Other radiation tests carried out with these devices have been described previously.<sup>5-8</sup> Three different spectra (Fig. 5) were obtained through the selection of various filters. Pulse widths ranged from 10 to 100 nsec, and peak dose rates from  $2 \times 10^7$  to  $4 \times 10^9$  rad(Si)/sec.

Two transistors and a PIN photodiode were mounted on a test fixture that was positioned 40 cm from the x-ray source to permit the simultaneous irradiation of all three devices by the plasma focus. Lead shielding, coated with two layers of a low Z tape to minimize photoemission, surrounded the semiconductors in order to eliminate extraneous photoresponses from other components employed on the test fixture. A diagram of the experimental arrangement is shown in Fig. 6. This fixture was mounted in a test chamber that was routinely evacuated to  $10^{-2}$  Torr to eliminate air-ionization effects.

The electrical circuit used for testing the transistors during irradiation by the plasma focus is shown in Fig. 7. The primary photocurrent  $I_{pp}$  was measured by opening the emitter and grounding the base lead ( $R_B = 0$ ). Similarly, the secondary photocurrent  $I_{sp}$  was measured with the emitter grounded and with various values of  $R_B$ . The currents were measured by fast-response, miniature-current transformers that were shielded appropriately. An electrical background noise of less than 1 mV was measured at peak dose rates. The incident dose rate on the transistors was measured with a PIN photodiode. The diode, with an area of  $0.014 \text{ cm}^2$  and thickness of 0.002 cm, had filtering identical to that used on the test transistor except that the filters were coated with low Z tape to prevent dose enhancement.

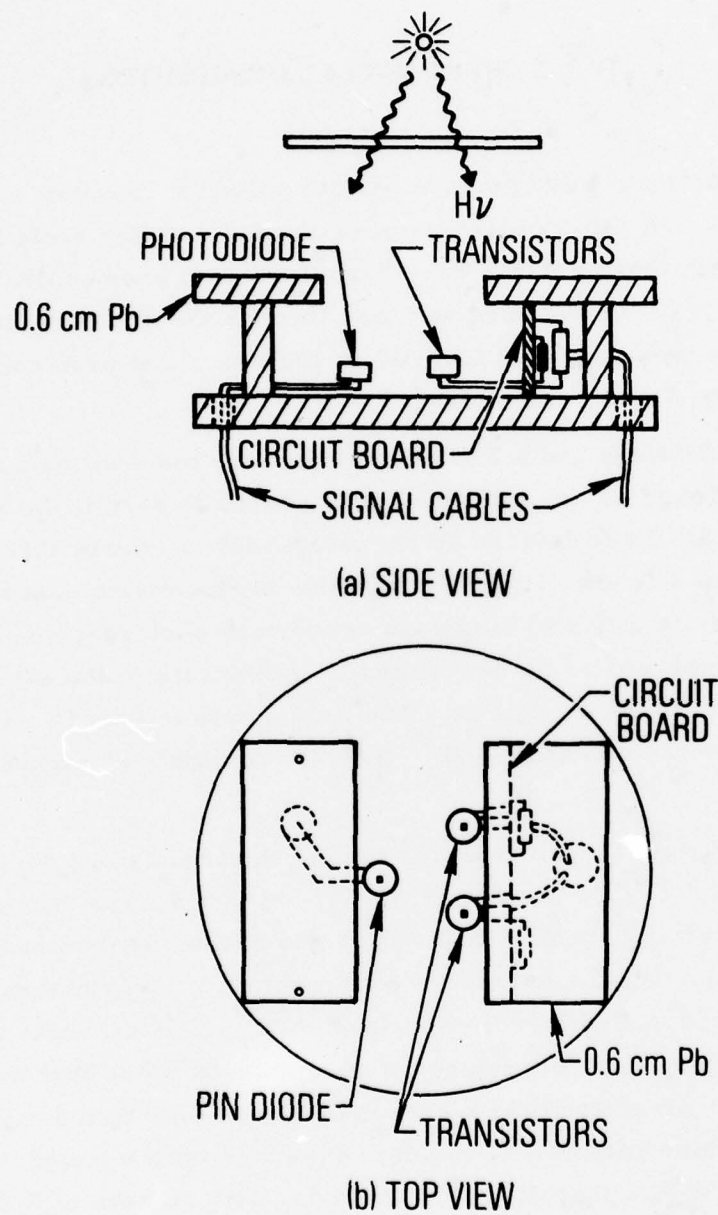


Fig. 6. Layout of Radiation-Response Test Fixture

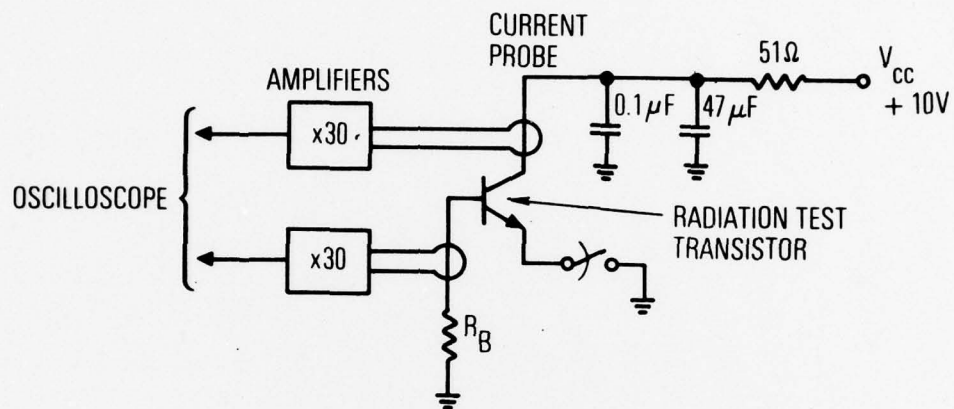


Fig. 7. Electrical Circuit for Radiation Tests

## V. RADIATION STUDIES

The transistors selected for the radiation studies were the 2N1613 and the 2N3947, which are both epitaxial type NPN. The criteria for selection, although somewhat arbitrary, were that the devices have a good high-frequency response and a simple geometry such that the relative areas could be easily calculated, that the transistors be of the general purpose variety, and that the device specifications readily available. The relevant characteristics of the two transistors obtained from the manufacturer as well as the specifications for the photodiode are given in Table 1.

Table 1. Device Characteristics

Device	2N1613	2N3947	Photodiode
Manufacturer	Motorola	Motorola	Quantrad
Type	NPN	NPN	PIN
Construction	Epitaxial	Epitaxial	Epitaxial
Geometry	Star	Rectangular	Rectangular
Collector area $A_c$ , $\text{cm}^2$	0.0014	0.00046	0.015
Collector diffusion length $L_c$ , cm		0.003	
Collector epitaxial thickness $W_t$ , cm	0.001	0.0009	0.002 <sup>a</sup>
Collector impurity concentration $N_c$ , atoms/ $\text{cm}^3$	$1 \times 10^{15}$	$2 \times 10^{15}$	
Base area $A_B$ , $\text{cm}^2$	0.0012	0.0003	
Base depth $r_j$ , cm	0.0003	0.0003	
Package			

<sup>a</sup>Thickness of active region of diode.

#### A. PHOTOCURRENT RESPONSE WITHOUT DOSE ENHANCEMENT

An initial study was made to determine the photocurrent response of the two devices from primary photoemission without the enhancement resulting from secondary photoemission, which was accomplished experimentally by modifying the transistor package before it was irradiated by the dense-plasma focus. Three modifications were used, which include: (1) the removal of the transistor Kovar lid, (2) the evacuation of the transistor package and back-filling with vacuum pump oil, and (3) the insertion of a low Z dielectric between the transistor lid and the semiconductor chip. Experimental tests indicated that the three methods were equally effective. These tests were conducted with the test fixture in a vacuum chamber; however, the results of additional tests with the fixture at atmospheric pressure were within 20% of those conducted in a vacuum, which suggests that air effects do not significantly affect the primary photocurrent response.

Shown in Figs. 8 and 9 are the results of these radiation studies with the DPF used as a photon source for the 2N3947 and 2N1613 transistors, respectively. Note that the data identified with solid circles correspond to the grounded-base, open-emitter configuration and represents the primary photocurrent  $I_{pp}$ . As expected from Eq. (1), this response varies linearly with the dose rate. The other data, which are appropriately identified, correspond to a configuration with the emitter grounded and a resistance  $R_B$  inserted in the base circuit. Only radiation pulses with durations greater than 50 nsec were considered so that steady-state approximations could be made.

The results of the primary photocurrent measurement are compared with the computed responses at a dose rate of  $10^8$  rad(Si)/sec in Table 2. The computed steady-state primary photocurrent responses from Eqs. (1) and (2) were in excellent agreement with the experimental results and are shown as a function of dose rate as dashed curves in Figs. 8 and 9.

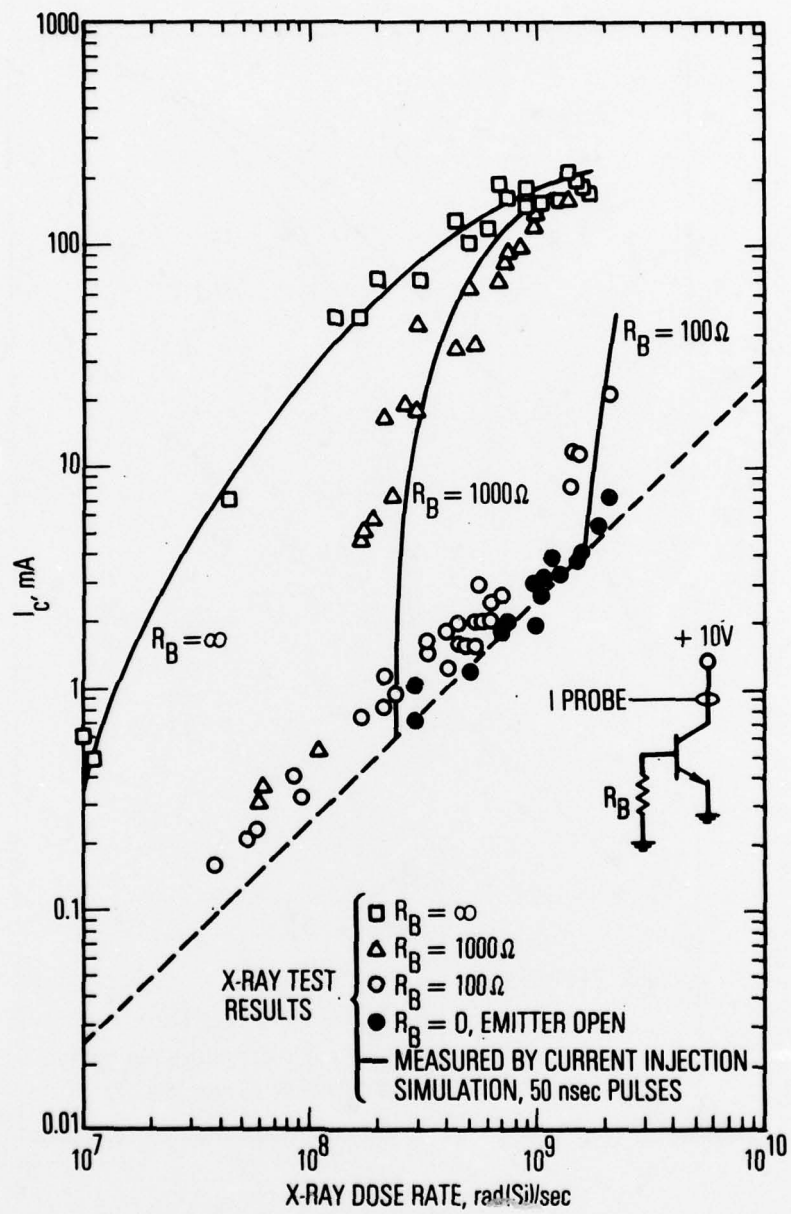


Fig. 8. Radiation Test Results for 2N3947 Transistor

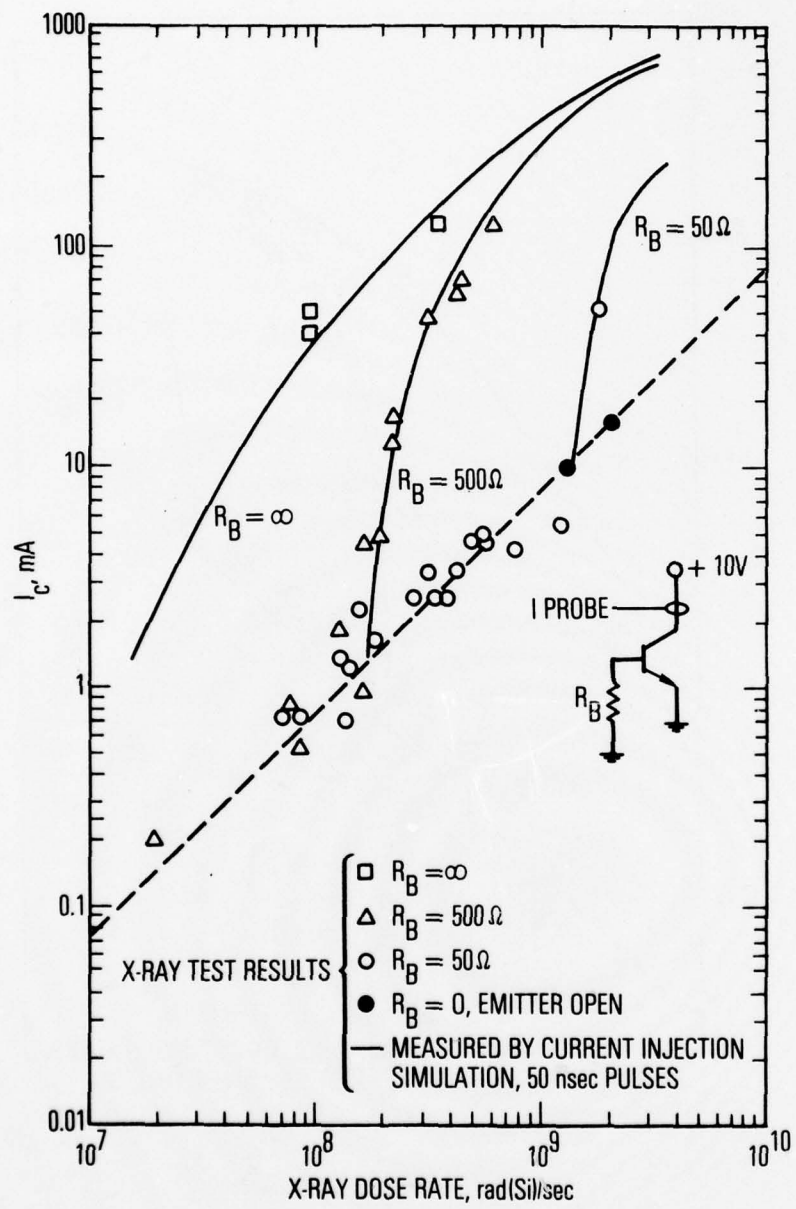


Fig. 9. Radiation Test Results for 2N1613 Transistor

Table 2.  $I_{pp}$  at  $10^8$  rad(Si)/sec Without Dose-Enhancement Effects

Transistor	2N1613	2N3947
Calculated $I_{pp}$ , mA	0.76	0.25
Measured $I_{pp}$ , mA	$0.80 \pm 0.2^a$	$0.27 \pm 0.09^b$

<sup>a</sup>Maximum spread of nine measurements.

<sup>b</sup>Maximum spread of 15 measurements.

The validity of the secondary photocurrent response was measured with the circuit shown in Fig. 10 to inject current pulses into the base of the test transistors in order to simulate the primary photocurrent. This injection circuit has a very large output impedance and provides a nearly constant current output for the pulse duration of 50 nsec. These data are shown in Figs. 8 and 9 as solid curves for the various base resistance considered. The injection base current is related to the incident dose rate by the calculated response for  $I_{pp}$  (dashed curves). Note, from the figures, that there is good agreement between the two methods.

#### B. PHOTOCURRENT RESPONSE WITH DOSE ENHANCEMENT

The enhancement in the photocurrent resulting from secondary emission from Z foils was investigated by comparing the responses from two matched semiconductors with identical filtration. With one device, the high Z foil was placed adjacent to the semiconductor; with the other device, a 0.005-cm polyethylene disk was placed between the foil and the semiconductor. This thickness of polyethylene was adequate to prevent electrons from reaching the chip after being emitted from the high Z foil. The high Z materials investigated were the Kovar lids from the transistor cans, which consist primarily of nickel and a  $5 \times 10^{-4}$  cm tantalum foil. Similar studies were performed with the  $2 \times 10^{-3}$ -cm-thick PIN diodes.

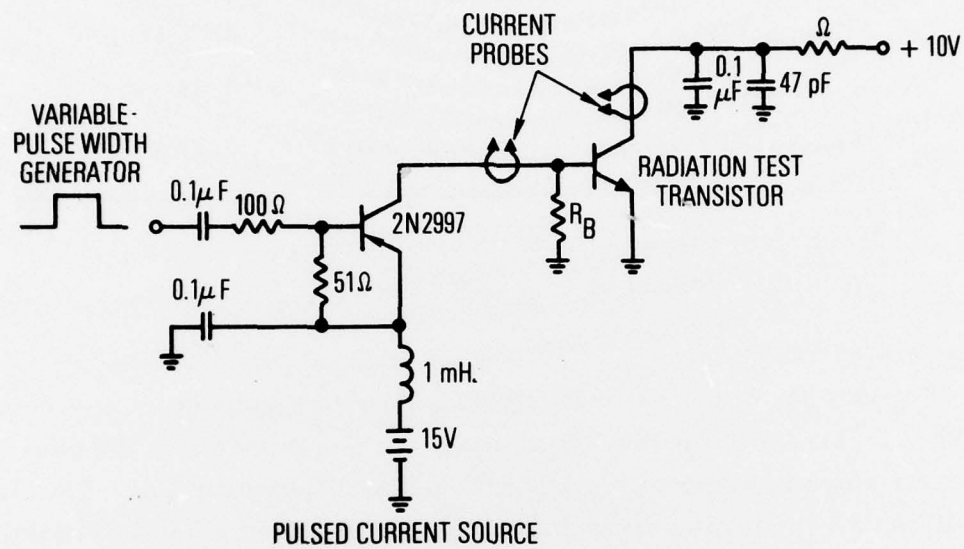


Fig. 10. Current Injection Circuit and Test Transistor

The primary photocurrents were measured for these configurations for each of the three spectra shown in Fig. 5. The dose-enhancement factor was calculated as the ratio of the primary photocurrents of the two devices being compared. The experimental results for the two transistors and the photodiode are listed in Table 3 for the three spectra.

Table 3. Measured Dose-Enhancement Factors

Device	Lid	Spectrum I	Spectrum II	Spectrum III
2N3947	Kovar	$1.6 \pm 0.2$	$2.2 \pm 0.3$	$1.7 \pm 0.3$
	Ta	$2.1 \pm 0.3$	$3.2 \pm 0.6$	$4.6 \pm 0.7$
2N1613	Kovar	$1.8 \pm 0.4$	$2.0 \pm 0.3$	$2.3 \pm 0.3$
	Ta	$2.0 \pm 0.2$	$3.2 \pm 0.4$	$4.1 \pm 0.7$
$2 \times 10^{-3}$ cm PIN Diode	Kovar	$1.2 \pm 0.1$	$1.2 \pm 0.1$	$1.2 \pm 0.2$
	Ta	$1.5 \pm 0.1$	$1.7 \pm 0.2$	$2.1 \pm 0.2$

Additional dose-enhancement data are also presented in Fig. 11 for the 2N1613 transistor in the amplifying mode, i.e., the emitter is grounded, and the base is connected to ground through a 1000- $\Omega$  resistor. In this study, a tantalum photoemitter and the DPF spectrum identified as Spectrum I in Fig. 5 were used. The dose rate, which is no longer linearly related to the transistor current, was measured by the PIN diodes.

#### C. COMPARISONS OF CALCULATED AND MEASURED DOSE-ENHANCEMENT FACTOR

The dose-enhancement factor for the transistors was calculated with the use of Eq. (4) and the depth-dose profiles of Figs. 3 and 4 in order

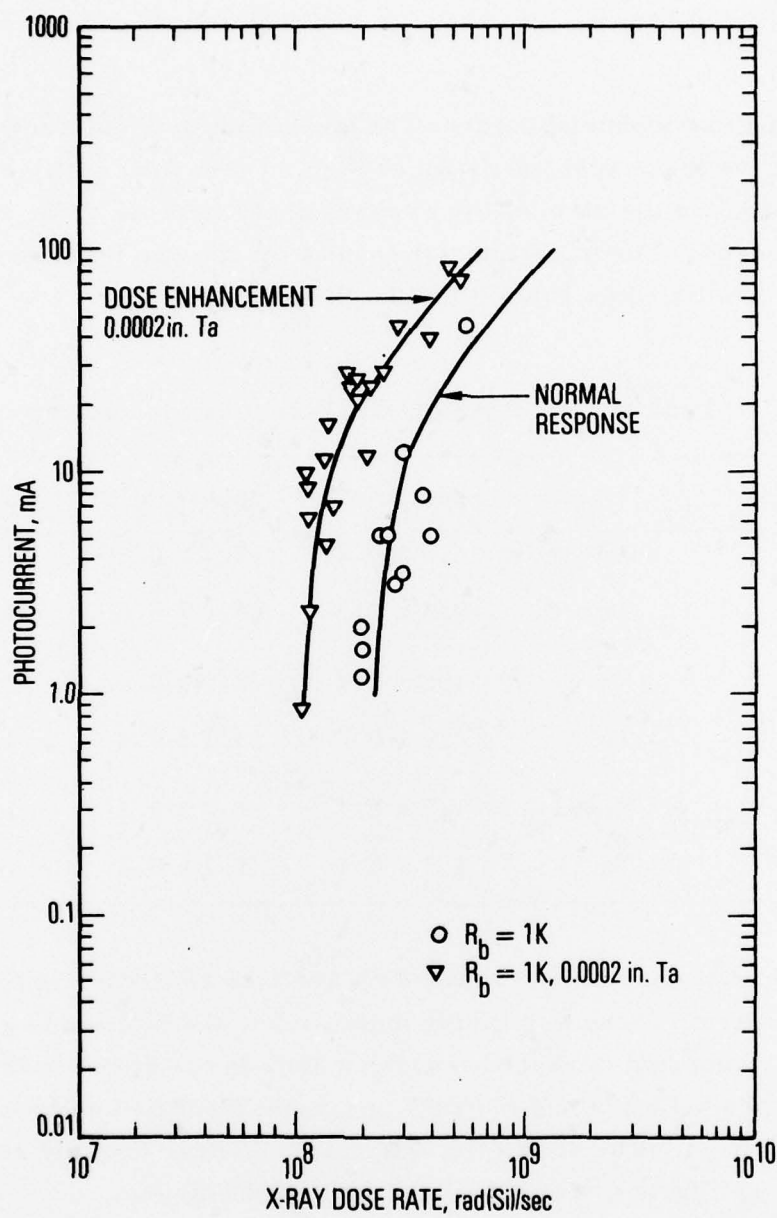


Fig. 11. 2N1613 Dose-Enhancement from  
0.0002 in. Ta with Spectrum I  
(0.4 cm Al filtration)

to define the secondary radiation function  $S(x)$  for nickel (Kovar) and tantalum, respectively. The integration limits of  $x_1 = 0.0003$  cm and  $x_2 = 0.0011$  cm define the boundaries of the active volume, with it assumed that there is a  $0.0001$ -cm  $\text{SiO}_2$  layer over the epitaxial silicon and that the first  $0.0002$  cm of silicon does not contribute to the primary photocurrent  $I_{pp}$ . The DEF was calculated to be 2.6 and 4.7 for the nickel and tantalum photoemitters, respectively, for the primary radiation, Spectrum I of Fig. 5.

In the calculations for the DEF for the  $0.002$ -cm PIN photodiode the same considerations as above were used; however, the integration limits were specified to be  $0.0003$  to  $0.0023$  cm. The dose-enhancement factors for the photodiode were calculated as 1.9 for nickel and 3.1 for tantalum.

All of the calculated values are higher than the actual measured values summarized in Table 3 for Spectrum I. Possible causes of error are (1) inaccurate specification of the spectrum for the depth-dose calculation, (2) failure to take into account the gap between the semiconductor chip and the photoemitting surface, (3) attenuation of photoelectrons by conducting pads and lead wires, and (4) inaccurate specification of the integration limits  $x_1$  and  $x_2$ .

## VI. CONCLUSION

The response of bipolar transistors to ionizing radiation consists of three contributing factors: (1) the primary photocurrent  $I_{pp}$ , (2) the secondary photocurrent  $I_{sp}$ , and (3) the dose-enhancement factor DEF. It was shown that  $I_{pp}$  can be predicted accurately by computations made on the basis of device geometry, whereas  $I_{sp}$  can be determined with the aid of simple bench tests. The dose-enhancement factor, however, is not as easily calculated, even with the aid of complex computer codes such as POEM, because parameters are involved that are difficult to measure when the incident radiation has low energy (20 to 100 keV). The depth-dose profile of the secondary electrons falls off very rapidly in silicon so that both the active volume of the transistor and the spectrum profile must be known precisely in order to obtain a reasonably accurate result. Thus, it is concluded that the transient low-energy radiation response of a transistor is best determined by laboratory simulation with a suitable radiation source.

# REFERENCES

1. D. M. Long and D. H. Swant, AFCRL-TR-74-0283, General Re-Entry and Environmental Systems Division, Electric Co., Philadelphia, Pa. (1974).
2. R. A. Berger and J. L. Azarewicz, IEEE Trans. Nucl. Sci. NS-22, 2568 (1975).
3. F. Larin, Radiation Effects in Semiconductor Devices, John Wiley and Sons, New York (1968).
4. W. L. Chadsey, AFCRL-TR-75-0324, Science Applications, Inc., McLean, Va. (1975).
5. F. Hai and M. J. Bernstein, IEEE Trans. Nucl. Sci. NS-18, 178 (1971).
6. M. J. Bernstein, IEEE Trans. Nucl. Sci. NS-20, 58 (1973).
7. R. H. Vandre, IEEE Trans. Nucl. Sci. NS-20, 180 (1973).
8. M. J. Bernstein and K. W. Paschen, IEEE Trans. Nucl. Sci. NS-21, 284 (1974).
9. M. J. Bernstein and K. W. Paschen, X-Ray Photoemission from Coated Surface, TR-0076(6124)-2, The Aerospace Corp., El Segundo, Calif. (19 December 1975).

## APPENDIX

COMPARISON WITH A HIGH-ENERGY  
RADIATION SOURCE

Tests were conducted in March 1974 as a cooperative effort between TRW and The Aerospace Corporation to determine the dose-enhancement effects resulting from photoemission from Kovar lids. Laboratory measurements of a Motorola Type 2N2944 with and without a 0.015-cm polyethylene insert between the lid and semiconductor chip were performed both on the Aerospace 34-kJ plasma-focus device and the TRW Febetron flash x-ray devices (2 MV). Theoretical support was provided by TRW. TRW calculated that the polyethylene insert would reduce the photoemission from the inside of the Kovar lid by a factor of 129 for the dense-plasma-focus spectrum, which, from Eq. (4), means that the integrated dose-depth profile  $S(x)$  would be reduced by a factor of 129 and the DEF would be reduced accordingly, depending on the magnitude of the primary dose  $P(x)$ . In the laboratory measurements, the primary photocurrent  $I_{pp}$  of the 2N2944 was reduced by a factor of 2 with the polyethylene inserted when the Aerospace dense-plasma focus source, with Spectrum I of Fig 3 used, generated the primary radiation spectrum. Similar measurements made with the TRW Febetron as the primary radiation source indicated that there was no difference with or without the polyethylene insert. This result was as expected because of the much harder x-ray spectrum of the Febetron that generated secondary electrons that were too energetic to be stopped by the polyethylene, which illustrates the extreme dependence of the dose-enhancement factor upon spectral characteristics.

### THE IVAN A. GETTING LABORATORIES

The Laboratory Operations of The Aerospace Corporation is conducting experimental and theoretical investigations necessary for the evaluation and application of scientific advances to new military concepts and systems. Versatility and flexibility have been developed to a high degree by the laboratory personnel in dealing with the many problems encountered in the nation's rapidly developing space and missile systems. Expertise in the latest scientific developments is vital to the accomplishment of tasks related to these problems. The laboratories that contribute to this research are:

**Aerophysics Laboratory:** Launch and reentry aerodynamics, heat transfer, reentry physics, chemical kinetics, structural mechanics, flight dynamics, atmospheric pollution, and high-power gas lasers.

**Chemistry and Physics Laboratory:** Atmospheric reactions and atmospheric optics, chemical reactions in polluted atmospheres, chemical reactions of excited species in rocket plumes, chemical thermodynamics, plasma and laser-induced reactions, laser chemistry, propulsion chemistry, space vacuum and radiation effects on materials, lubrication and surface phenomena, photo-sensitive materials and sensors, high precision laser ranging, and the application of physics and chemistry to problems of law enforcement and biomedicine.

**Electronics Research Laboratory:** Electromagnetic theory, devices, and propagation phenomena, including plasma electromagnetics; quantum electronics, lasers, and electro-optics; communication sciences, applied electronics, semiconducting, superconducting, and crystal device physics, optical and acoustical imaging; atmospheric pollution; millimeter wave and far-infrared technology.

**Materials Sciences Laboratory:** Development of new materials; metal matrix composites and new forms of carbon; test and evaluation of graphite and ceramics in reentry; spacecraft materials and electronic components in nuclear weapons environment; application of fracture mechanics to stress corrosion and fatigue-induced fractures in structural metals.

**Space Sciences Laboratory:** Atmospheric and ionospheric physics, radiation from the atmosphere, density and composition of the atmosphere, aurorae and airglow; magnetospheric physics, cosmic rays, generation and propagation of plasma waves in the magnetosphere; solar physics, studies of solar magnetic fields; space astronomy, x-ray astronomy; the effects of nuclear explosions, magnetic storms, and solar activity on the earth's atmosphere, ionosphere, and magnetosphere; the effects of optical, electromagnetic, and particulate radiations in space on space systems.

THE AEROSPACE CORPORATION  
El Segundo, California